Phenotypic Covariation And Morphological Diversification In The Ruminant Skull

Annat Haber

University of Chicago, Committee on Evolutionary Biology, Chicago, IL

Dept. of Zoology, Tel Aviv University, Tel Aviv, Israel

Current address:

Michigan State University, BEACON Center for the Study of Evolution in Action

567 Wilson Rd, room 1450, East Lansing, MI 48824

annat22@gmail.com

Online Appendix A: Additional details on methods and results

Online Appendix B: Simulations exploring the relationship between Average flexibility and rSDE

Dryad files: Data, phylogenetic hypotheses, and annotated R codes for all analyses

Submitted as an article

April 2015

1   Abstract

2   Differences between clades in their diversification patterns result from a combination of extrinsic

3   and intrinsic factors. In this study I examined the role of intrinsic factors in the morphological

4   diversification of ruminants in general, and in the differences between bovids and cervids in

5   particular. Using skull morphology, which embodies many of the adaptations that distinguish

6   bovids and cervids, I examined 132 of the 200 extant ruminant species. As a proxy for intrinsic

7   constraints I quantified different aspects of the phenotypic covariation structure within species,

8   and compared them with their among-species divergence patterns, using phylogenetic

9   comparative methods. My results show that bovids have dispersed into a wider range of directions

10   in morphospace than cervids, and that their overall disparity is higher. Within both bovids and

11   cervids, most species divergence is well aligned with their phenotypic covariance matrices, and

12   those that are better aligned have diverged further away from their ancestor. Bovids' greater

13   disparity and broader dispersion is associated with a lower eccentricity of their within-population

14   covariance matrices. These results are consistent with the role of intrinsic constraints in

15   determining amount, range, and direction of dispersion, and demonstrate that intrinsic constraints

16   can influence macroevolutionary patterns even as the covariance structure evolves.

17

Introduction

Diversity is distributed unevenly across the tree of life; a fact that is at the heart of many research programs in evolutionary biology. This unevenness is the result of both extrinsic and intrinsic factors. While extrinsic factors provide the opportunities for diversification, intrinsic factors determine the variation available for natural selection to work on, and therefore the potential of the population to respond to environmental changes and to take advantage of these opportunities. Studying this potential is therefore crucial for understanding macroevolutionary patterns. A common approach for studying the effect of intrinsic factors is to look at the structure of phenotypic and genetic (co)variation within the population, and compare it to patterns of divergence among populations (Lande 1979; Zeng 1988; Armbruster 1996; Schluter 1996; Arnold et al. 2001; Ackermann and Cheverud 2002; Hansen and Houle 2008; Hohenlohe and Arnold 2008; Marroig et al. 2009; Bolstad et al. 2014). In this study I examine the role of phenotypic covariation and intrinsic constraints in the morphological diversification of the ruminant skull, with particular emphasis on the contrast between bovids and cervids.

According to the quantitative genetics framework (Lande 1979), the rate and direction of short-term evolution depends on the relative alignment between selection and the within-population genetic (**G**) and phenotypic (**P**) covariation, as well as their strength. A closer alignment between the major axis of covariation and selection allows the population to evolve more rapidly in the direction of selection because more variation is available in this direction. A greater angle between them will divert the population further away from the optimum, slowing down its evolution. A direct extension of this framework to the macroevolutionary scale predicts that the divergence of populations will initially be biased by the major axis of their ancestral covariation structure – resulting in a close alignment between the within-population covariation and the

3

40   among-population divergence – and that this effect will diminish with time (Zeng 1988; Armbruster

41   1996; Schluter 1996).

42   Hansen and Houle (2008) expanded this approach to quantify different aspects of the

43   evolutionary potential and provide a null expectation for evaluating the extent of the bias (Hansen

44   and Voje 2011; Bolstad et al. 2014). They defined the evolvability of a single trait as the expected

45   change in trait value in response to directional selection of unit strength per generation, measured

46   as the mean-scaled trait variance. In a multivariate space, evolvability can vary in different

47   directions and is therefore defined with respect to a specific direction; e.g., that in which selection

48   is acting or that in which divergence has occurred ($e(\mathbf{d}_{SP})$ and $e(\mathbf{d}_{CL})$; see table 1 for details). The

49   conditional evolvability is defined as the expected change in a given direction assuming stabilizing

50   selection in the remaining directions, thus accounting for trait covariances as well as variances.

51   When averaged across random directions these measures provide the null expectation of no bias

52   ($\bar{e}$ and $\bar{c}$ in table 1).

53   At both the micro- and the macro-evolutionary scales, this framework has focused on the

54   relative alignment between covariation and selection. It measures the amount of variation

55   available in a specific direction and therefore the potential to evolve faster in that direction.

56   However, as the phylogenetic scale and time span of the study increase it becomes more difficult

57   to reconstruct selection and covariation at any given time, and more likely that either or both have

58   changed repeatedly, so that their average estimation (or ancestral reconstruction) becomes less

59   informative. The stability and predictability of **P** and **G** has been a particularly thorny issue when

60   attempting to bridge the micro and macro scales, with the growing understanding that the relevant

61   question is when and how they evolve, rather than if, and that the answer is complex and context-

62   dependent (Arnold et al. 2008; Haber 2015; and references therein). Moreover, on the macro

63   scale, selection is more likely to have shifted often enough and in directions different enough

64   (Uyeda et al. 2011; Jones et al. 2012), presenting the populations with a more diverse array of

65   challenges and opportunities. The probability of going extinct or being outcompeted before

66   reaching the optimum also becomes increasingly relevant (Jablonski 2007; Gomulkiewicz and

67   Houle 2009; Jones et al. 2012). Therefore, we might expect that the long-term evolutionary success

68   of lineages and clades would be largely determined – and therefore better predicted – by their

69   ability to respond effectively to a wide range of selective pressures (Vermeij 1973; Liem 1973;

70   Draghi and Wagner 2008), rather than their ability to respond faster in any particular direction. In

71   this context, 'responding effectively' means reaching close enough to the optimum to avoid

72   extinction or competitive displacement, until selection changes again.

73   I consider here four measures that could reflect the potential to respond to a wide range of

74   selective pressures: $\bar{e}$, $\bar{c}$, $\bar{f}$, and rSDE($\mathbf{P}$) (see table 1 for details). The average evolvabiliy ($\bar{e}$) and

75   conditional evolvabiliy ($\bar{c}$) developed by Hansen and Houle (2008) measure the variance available

76   in any random direction on average, and thus the average potential to respond to any selection

77   vector. A higher value of $\bar{e}$ or $\bar{c}$ can be interpreted as a greater potential to respond to a wider

78   range of selection vectors, where $\bar{c}$ accounts also for the possibility of stabilizing selection in the

79   remaining directions. Both are proportional to total variance (i.e., matrix size), and $\bar{c}$ accounts also

80   for trait covariances (i.e., matrix shape). Another measure developed based on Hansen and Houle

81   (2008) is the average flexibility ($\bar{f}$; Marroig et al. 2009; Roland 2009), which measures how much

82   the population response is deflected from the direction of selection, on average. A higher value

5

83   means that the population is less biased by its major axis of covariation and is able to align more

84   closely with a wider range of selection vectors (i.e., more flexible). $\overline{f}$ quantifies matrix shape only,

85   not accounting for the orientation and size of the matrix.

86   Another metric that quantifies matrix shape only, albeit in a different way, is the relative

87   standard deviation of the eigenvalues (rSDE($\mathbf{P}$) in table 1). This metric, and its variations, has been

88   referred to as integration level in studies of morphological integration (Wagner 1984, Cheverud et

89   al. 1989, Pavlicev et al. 2009, Haber 2011). Its use as a measure of integration has been criticized

90   recently for being merely descriptive with no link to the theory of integration and evolution

91   (Armbruster et al. 2014). However, here I use it to quantify matrix shape – as originally suggested

92   by Van Valen (1974) – and reinterpret it in the context of Hansen and Houle's (2008) model. Since

93   evolvability is defined as the (mean-scaled) variance in a given direction, the eigenvalues of a

94   matrix measure the evolvabilities along its eigenvectors. Therefore, rSDE($\mathbf{P}$) measures the variation

95   in the ability to respond in different directions. Because rSDE($\mathbf{P}$) is standardized by the total

96   variance of the matrix, it captures matrix shape only. When the variation in the sample is

97   distributed more evenly in different directions, matrix shape is less eccentric, and rSDE($\mathbf{P}$) is lower.

98   By definition, matrices with a lower eccentricity are less biased by their major axis of covariation.

99   Therefore, we would expect rSDE($\mathbf{P}$) to have a tight negative correlation with $\overline{f}$. Indeed,

100   preliminary simulations indicate that this relationship persists for a wide range of matrices that

101   differ in their number of variables, mean correlation, and heterogeneity (see online appendix B).

102   To the extent that the observed covariation matrix reflects underlying integrating factors, a more

103   eccentric matrix would reflect a body-plan that is more strongly integrated overall. However, the

6

104   link between rSDE(**P**) and integration is not the focus of this study. Instead, I focus here on the link

105   between rSDE(**P**) and macroevolution.

106   Which variational property best predicts macroevolutionary patterns is still an open

107   question (Hansen 2012; Bolstad et al. 2014). Because $\bar{e}$ and $\bar{c}$ are proportional to matrix size (i.e.,

108   total variance), a direct extrapolation to macroevolution assumes a linear relationship between the

109   probability of responding effectively and the variance available to selection at any given time. We

110   might, however, imagine a situation where the relationship is not linear, involving a threshold of

111   variance that needs to be exceeded in order to avoid extinction and/or diverge successfully. When

112   the variation is distributed more evenly across the different dimensions, there would be more

113   directions in which the threshold is likely to be exceeded (for a given matrix size). Therefore, for a

114   given matrix size, a population with a lower eccentricity would be able to respond effectively in

115   more directions, and would be more likely to persist, evolve, and diversify in the long run,

116   regardless of its orientation. This prediction relies on several additional assumptions (see

117   *Discussion*). The extent to which they are warranted in practice and under what conditions is not

118   known, and developing and exploring a comprehensive quantified model is beyond the scope of

119   this study. Here I explore an empirical case in which these additional considerations are likely to be

120   relevant.

121   Ruminants comprise the bulk of Artiodactyla (Vrba and Schaller 2000; Theodor et al. 2005),

122   and consist of Tragulidae (chevrotains) and Pecora (giraffes, pronghorn, musk deer, bovids, and

123   cervids). Bovids and cervids are currently the most species-rich families within Ruminantia (143

124   and 51 extant species, respectively). Yet, their taxonomic richness is not too high to be reasonably

125   sampled within the scope of this study, allowing for both good taxonomic coverage and large

7

126   within-species samples. In addition, their phylogenetic history is relatively well understood

127   (Hernández Fernández and Vrba 2005; Price et al. 2005; Gilbert et al. 2006; Marcot 2007;

128   Agnarsson and May-Collado 2008; Decker et al. 2009). Their fossil record is exceptionally good for

129   vertebrates (Geist 1985, 1987; Janis 1989; Vrba and Schaller 2000; Marcot 2004; Pitra et al. 2004;

130   Ropiquet and Hassanin 2005; Theodore et al. 2005; Gillbert et al. 2006; Janis 2008; Heywood

131   2010), providing ample evidence that ruminants have faced a wide range of selective pressures

132   due mostly to global changes such as Plio-Pleistocene glacial cycles and the opening of grasslands.

133   At the same time, the fossil record reveals that cervids have had about the same opportunities as

134   bovids to exploit open habitats and arid grasslands at least since the late Miocene (Janis 2008;

135   Heywood 2010). Yet, no cervid has evolved into a true grazer. Cervids are mostly browsers,

136   occupying habitats with dense vegetation, whereas bovids exhibit a high diversity of feeding

137   adaptations and a wider range of body size and shape (Allard et al. 1992; Spencer 1997; Sinclair

138   2000; Marcot 2004; Janis 2008; Heywood 2010). These differences have left researchers puzzled as

139   to why cervids have not taken advantage of the same opportunities as bovids (Janis 2008;

140   Heywood 2010). My results support the role of intrinsic constraints in the morphological

141   diversification of both bovids and cervids, and suggest that the greater diversification of bovids is

142   best explained by their lower within-population eccentricity. I discuss these results in the context

143   of ruminant history and the extrapolation from micro- to macroevolution.

144

145   Materials and Methods

146   ***Data collection and preparation***

147   A total of 2857 skulls were included in this study, representing 5 out of 8 species of

148   tragulids, 3 out of 7 extant species of moschids, 34 out of 51 extant species of cervids, and 87 out

149   of 143 extant species of bovids. All 19 extant cervid genera are represented except *Przewalskium*

150   *albirostris*, which has been endangered for the last few decades. Of the 50 extant bovid genera, 40

151   are represented. The remaining 10 consist of only 1 to 3 species each and are all nested within

152   otherwise well-represented clades. All domesticated species were excluded. Taxonomic

153   assignments of specimens were standardized following Grubb (2002). Only prime age adults were

154   measured, as determined by their dentition and cranial sutures. Three-dimensional coordinates

155   were recorded for 43 landmarks using MicroScribe MLX (online table A1). Landmark definition was

156   based on the standard measurements recommended by von den Driesch (1976), as well as other

157   studies of the artiodactyl skull (Janis 1990; Mendoza et al. 2002; Semprebon et al. 2004). Data

158   processing involved unifying the dorsal and ventral aspects of the skull, averaging the left and right,

159   and identifying outliers (see online Appendix A for details). Variances due to measurement error,

160   were found to be between 1 to 3 orders of magnitude lower than the inter-specimen variance (see

161   online Appendix A).

162   Two datasets of interlandmark distances were created. For the first set ('ILtes'), 107

163   interlandmark distances were defined based on Delaunay tessellation of the symmetric mean

164   configuration of all specimens, function *delaunayn* in the R package *geometry* (Barber et al. 2012).

165   This procedure maximizes coverage while minimizing redundancy and crossing over spatial

166   modules. The second set ('IL32') included 32 ILMDs selected based on comparability with other

9

167   studies (e.g., von den Driesch 1974; Janis 1990; Marroig and Cheverud 2004; Mendoza et al. 2002)

168   and interpretability in the context of either function or putative modules (see online table A2).

169   Both datasets were corrected for variation due to subspecies and sex by adding to each value

170   within a subsample the difference between the grand mean and the subsample mean (Sokal and

171   Rohlf 1995; Marroig and Cheverud 2004). No significant effect of sex and subspecies was found on

172   either the orientation or eccentricity of the covariance matrix for most species. Species for which I

173   found a substantial effect, even if non-significant, were reduced to the largest single subspecies

174   sample. A MANOVA test revealed no significant interaction between sex and subspecies for mean

175   shape.

176   ***Quantifying within-population covariation***

177   A **P** matrix was calculated for each species with more than 27 specimens, including 2

178   species of tragulids, 13 species of cervids, and 32 species of bovids (see fig. 2 for details). Three

179   subspecies of white-tailed and mule deer were analyzed separately, bringing the total number of

180   cervid samples to 17. Variables were scaled by the species mean. Scaling by the mean mitigates the

181   isometric effect of size variation among individuals (within and across species), as well as scale

182   differences among variables, and ensures that the evolvability measures are meaningful in the

183   context of Lande's (1979) equation (Hansen et al. 2011). A non-weighted bending procedure was

184   applied to each matrix to ensure that it is positive-definite (Jorjani et al. 2003; Pavlicev et al. 2009).

185   Each sample was jackknifed specimen-by-specimen to identify aberrant specimens.

186   The average evolvability ($\bar{e}$), average conditional evolvability ($\bar{c}$), and average flexibility ($\bar{f}$)

187   were calculated using simulations of random selection vectors (Marroig et al. 2009; Rolian 2009;

188   Bolstad et al. 2014; see table 1). rSDE(**P**) was calculated based on the eigenvalues (see table 1) and

189   adjusted for the effect of sample size by subtracting the mean of a 1000 permutations from the

190   observed value. This is equivalent to the correction suggested by Wagner (1984), but applicable to

191   covariances as well as correlations. Confidence intervals were estimated using a non-parametric

192   bootstrap procedure with a bias correction (BCa; DiCiccio and Efron 1996; Carpenter and Bithell

193   2000) and 999 iterations. The BCa correction was necessary because the pseudovalues distribution

194   is expected to be biased upward and to depend on its mean when bounded by zero and/or one.

195   The evolution of rSDE(**P**), ($\overline{e}$), and ($\overline{c}$) was explored by fitting several Ornstein-Uhlenbeck

196   models, as well as a Brownian motion model, in order to identify nodes where a shift in the clade's

197   typical values has occurred (interpreted here as selective regime; Hansen 1997; Butler and King

198   2004). Using R package *maticce* (Hipp and Escudero 2010), I tested five nodes: all ruminants

199   excluding tragulids (node number 8 in Hernández Fernández and Vrba 2005); Bovidae (node 15);

200   Cervidae (node 25); Cervinae (node 27); and Caprinae (node 139). All possible combinations of the

201   five putative transitions were tested, resulting in 32 alternatives of the OU model and one

202   Brownian motion model (see table 2). Values were ln-transformed for this analysis, and branch

203   length was scaled by tree height. Models were selected based on the relative weights of their AICc

204   scores (Anderson et al. 2000). The maximum likelihood estimate for each regime was estimated as

205   an average of the 32 models, weighted by their AICc weights (Anderson et al. 2000).

206   ***Quantifying morphological dispersion***

207   The among-population divergence was measured by the overall amount, rate, and

208   eccentricity of dispersion (table 1). These measures were calculated separately for each clade –

209   Bovidae, Cervidae, Cervinae, and Caprinae, as above – based on its species means. Species means

210   were scaled by the clade's phylogenetically-weighted mean (the inferred root state), assuming a

11

211   Brownian motion model (function *fastAnc* in the R package *phytools*; Revel 2012). The overall

212   dispersion was calculated as the mean squared morphological distance between each species and

213   the clade's phylognetically-weighted mean (equivalent to Foote 1993's disparity). To facilitate

214   comparisons, the expected distribution under Brownian motion model was generated by

215   simulating a 1000 datasets (function *sim.char* in the R package *Geiger*; Harmon et al. 2008) and

216   recalculating disparity for each simulated dataset. The rate parameters for these simulations were

217   provided by the clade's evolutionary rate matrix ($\mathbf{D}_{IC}$ in table 1). $\mathbf{D}_{IC}$ is the covariance matrix of

218   independent contrasts between species means, assuming a Brownian-motion model, and

219   therefore represents the coevolution of traits while taking into account phylogeny (Revell 2007;

220   Revell and Harmon 2008). The rate of dispersion is the trace of $\mathbf{D}_{IC}$. The eccentricity of dispersion is

221   the relative standard deviation of the eigenvalues of $\mathbf{D}_{IC}$ (rSDE($\mathbf{D}_{IC}$) in table 1). Thus, this metric

222   measures how evenly species have diverged in morphospace. Confidence intervals for the rates

223   and eccentricity of dispersion were estimated using a parametric bootstrap procedure with 500

224   replications, using the original sample size and assuming a multivariate normal distribution.

225   ***Evolvability in the direction of divergence***

226   Species divergence was compared with the amount of mean-scaled phenotypic variance

227   (evolvability) available in the direction of divergence, following Hansen and Houle (2008) and

228   Hansen and Voje (2011). I first calculated the amount of variation that each species has along the

229   eigenvectors of its clade's evolutionary rate matrix ($e(\mathbf{d}_{CL})$; see table 1 for details), using its

230   observed **P**. Species whose **P** matrices are more closely aligned with their clade's diversification

231   would have higher evolvabilities along the first eigenvector of $\mathbf{D}_{IC}$ than along other eigenvectors. I

232   then calculated the amount of variation available for species in the direction of their own

233   divergence from their clade's inferred root state (($e(\mathbf{d}_{SP})$ and $c(\mathbf{d}_{SP})$ in table 1; Hansen and Voje

234   2011), based on the clade's average **P** (**P**$_{AV}$). Ideally, **P** here would be averaged over the clade's

235   history while accounting for phylogeny. However, previous analyses (Haber 2015) indicated that

236   the phylogenetic structure of **P** within each clade has been obliterated substantially. Therefore, the

237   simple average – i.e., assuming 'white noise' model – was preferred over other evolutionary

238   models. The observed evolvabilities were compared to the expected values for random directions

239   ($\bar{e}$ and $\bar{c}$; table 1), also calculated here based on **P**$_{AV}$ (Hansen and Houle 2008, Hansen and Voje

240   2011). Higher evolvabilities indicate species that have diverged closer to the direction of **P**$_{AV}$ than

241   expected by chance (Hansen and Voje 2011).

242   All analyses were repeated for three different phylogenetic hypotheses derived from the

243   literature. Because results were essentially the same regardless of phylogeny, I present below

244   results based on the phylogeny of Hernández Fernández and Vrba (2005) only. Results based on

245   the other two phylogenies are presented in online appendix A. All analyses were carried out using

246   R v.3.0.2 (R development Core Team 2013). The phylogenetic trees were generated and

247   manipulated using packages *ape* (Paradis et al. 2004) and *phytools* (Revell 2012). All R scripts, data,

248   and phylogenetic hypotheses are available on Dryad (###).

249

250   Results

251   ***Within-population covariation***

252   The two datasets (ILtes, IL32) yield largely the same results (online fig. A3), indicating that

253   the smaller dataset captures most of the relevant information with its 32 variables. Values based

254   on the IL32 datasets are consistently lower than those based on the ILtes datasets, probably due to

255   a lower overall level of redundancy in the data, and the signal is often weaker. Adjusting rSDE($\mathbf{P}$)

256   for sample size has little effect (online fig. A4).

257   Average flexibility ($\bar{f}$) has a tight inverse correlation with the within-population eccentricity

258   (rSDE($\mathbf{P}$)); average evolvability ($\bar{e}$) is positively but loosely correlated with rSDE($\mathbf{P}$); and average

259   conditional evolvability ($\bar{c}$) is not correlated with rSDE($\mathbf{P}$), nor with $\bar{e}$ (fig. 1). $\bar{c}$ has yielded different

260   results depending on shrinking tolerance, method of matrix inversion, and number of variables

261   (online figure A3), and should therefore be regarded with caution. All rSDE($\mathbf{P}$) values deviate from

262   zero after adjusting for sample size (fig.2), indicating that all species deviate significantly from the

263   null expectation of a random covariation structure. Bovids are in general less variable than cervids

264   (fig. 2); most bovid species do not differ from each other substantially, with the striking exception

265   of Caprinae, whereas cervids show considerable variation throughout the clade and even among

266   conspecific subspecies.

267   The model fitting results indicate that rSDE($\mathbf{P}$) and $\bar{e}$ have not evolved following a Brownian

268   motion process, but rather as a multi-regime OU process (table 2). The most strongly supported

269   transition for rSDE($\mathbf{P}$) is at the base of Caprinae; all models that do not include a shift at this node

270   (models 17-32) have the lowest AICc weights. The best-supported model for all datasets (model 14

14

271 in table 2) includes a shift at the base of Cervidae as well as Caprinae. In addition, there is strong

272 evidence against a transition at the base of bovids plus cervids (node 8FV in table 2), as well as at

273 the base of all bovids. Therefore, bovids and cervids probably do not share the same typical

274 rSDE(**P**) value. Bovids and tragulids, on the other hand, have the same typical value, which most

275 likely characterized their ruminant ancestor as well. Model 10, which includes a shift for cervines in

276 addition to cervids and caprines, is also relatively well supported (see also online tables A3-A5).

277 Therefore, there is some evidence that the typical rSDE(**P**) value of cervines is higher than that of

278 other cervids. The best-supported model for $\bar{e}$ includes a transition for both bovids and caprines

279 (model 8) and none for other clades (table 2), implying that bovids have deviated from the

280 ancestral ruminant state rather than cervids.

281 Parameter estimates for the best-supported models are given in table 3, along with their

282 weighted averages. The shifts inferred for rSDE(**P**) involve an increase for caprines and cervids (and

283 possibly cervines). The shifts inferred for $\bar{e}$ involve a decrease for bovids and an increase for

284 caprines, relative to cervids and the ancestral state. The alpha estimates for rSDE(**P**) are high,

285 yielding a phylogenetic half-life of almost 8% of total tree height (calculated as log(2)/alpha;

286 Hansen 1997). This implies that half of the phylogenetic structure has been obliterated within less

287 than 4 My, out of the 50 My of ruminant history. The sigma-squared estimates for the best OU

288 models are about 4 times higher than that of the Brownian motion model, implying a very strong

289 stabilizing effect. The alpha and sigma-squared estimates are even higher for $\bar{e}$.

290 ***Morphological dispersion***

291 The position of both species of *Alces* in morphospace deviates substantially from all other

292 cervids (online fig. A2). Therefore, all measures were repeated for cervids with and without *Alces*.

293   Bovids' disparity is at the higher end of the expected range based on a Brownian motion model,

294   especially when caprines are excluded, whereas cervids' disparity is at the lower end, especially

295   when *Alces* is excluded (fig. 3). Bovids' rate of dispersion is somewhat lower than that of cervids,

296   although this difference is not significant and disappears when *Alces* is excluded (fig. 3). Cervids'

297   eccentricity of dispersion is significantly higher than that of bovids, especially when *Alces* is

298   excluded (fig. 3). Caprines' eccentricity and total disparity are lower than that of all bovids, but

299   their rate of dispersion is higher. These findings are somewhat more pronounced based on ILtes

300   and the alternative phylogenies (online figures A6-A7)

301   ***Evolvability in the direction of divergence***

302   Most species have substantially higher evolvabilities ($e(\mathbf{d}_{CL})$) along the first eigenvector of

303   their clade's evolutionary rate matrix, $\mathbf{D}_{IC}$, than along other eigenvectors (fig.4). The first

304   eigenvector is associated with 76%-85% of the variation in $\mathbf{D}_{IC}$. The minimal overlap between the

305   range of evovlabilities along the first eigenvector and those along other eigenvectors indicate that

306   the vast majority of species have their **P** matrix more closely aligned with their $\mathbf{D}_{IC}$ than expected

307   by chance. At the same time, the wide range of values along the first eigenvector indicates that

308   species differ greatly in their alignment. Cervids' median value is only slightly higher than that of

309   bovids, and their range is somewhat wider based on IL32 (though not based on ILtes; online fig.

310   A8). Caprines have the same median and range as bovids. Excluding caprines from bovids (online

311   fig. A10) and *Alces* from cervids (online fig. A11) made no difference.

312   Most of the observed evolvabilities in the direction of species divergence – $e(\mathbf{d}_{SP})$ and $c(\mathbf{d}_{sp})$

313   – are closer to the maximum value than to the expected value for random directions (fig. 5). The

314   average evolvability of $\mathbf{P}_{AV}$ is 0.31% of trait mean for bovids, 0.19% for cervids, and 0.06% for

315   caprines, whereas the observed $e(\mathbf{d}_{SP})$ are above 0.4%, 0.6%, and 0.29%, respectively. The average

16

316   conditional evolvability of $\mathbf{P}_{AV}$ is 0.08% for bovids, 0.05% for cervids, and 0.01% for caprines,

317   whereas all the observed $c(\mathbf{d}_{sp})$ are an order of magnitude higher. Many of the bovid $c(\mathbf{d}_{sp})$ values

318   are over 1%, whereas most cervid $c(\mathbf{d}_{sp})$ values are below 0.5%. When caprines are excluded from

319   bovids, all bovid $c(\mathbf{d}_{sp})$ values are lower than 1% (online fig A15). When *Alces* is excluded from

320   cervids, more $c(\mathbf{d}_{sp})$ values exceed 0.5% (online fig A17), thus narrowing the gap between bovids

321   and cervids.

322   There is a distinct non-linear association between the observed $e(\mathbf{d}_{sp})$ and $c(\mathbf{d}_{sp})$ values and

323   the amount of morphological divergence, d^2 (fig. 5). Species whose divergence is more closely

324   aligned with the direction of maximum evolvability managed to diverge further away from the

325   clade's ancestral state. The curve flattens close to the maximum value of evolvability at about

326   150% distance, in both bovids and cervids. Only species whose divergence is well aligned with the

327   direction of the major axis of their $\mathbf{P}_{AV}$ (i.e., their observed $e(\mathbf{d}_{SP})$ value is close to the maximum)

328   managed to diverge beyond that threshold.

17

329

330   Discussion

331   The role of intrinsic constraints in determining macroevolutionary patterns is still an open

332   question in evolutionary biology. The structure of variation and covariation within the population

333   has been used for studying the role of intrinsic constraints on generational scale, but it is still not

334   clear which properties of that structure best predict evolutionary outcomes on the macro scale,

335   and under what conditions. The question of why some clades are more diverse than others is of

336   particular interest for macroevolutionary studies. The contrast between bovids and cervids is such

337   an example. Previous studies have provided ample evidence that bovids are substantially more

338   diverse than cervids, taxonomically and ecologically (Allard et al. 1992; Spencer 1997; Sinclair 2000,

339   Grubb 2002; Marcot 2004; Janis 2008; Heywood 2010). Based on discrete characters of teeth,

340   Marcot (2004) has shown that bovids have been more diverse morphologically at least since the

341   late Miocene (about 10 Mya). Here I provide additional evidence – based on their skull morphology

342   – that bovids have a higher disparity than cervids and have dispersed into a wider range of

343   directions in morphospace. So far, studies of the fossil record have not been able to explain these

344   differences based on extrinsic factors (Janis 2008; Heywood 2010). My findings suggest that

345   intrinsic constraints have played an influential role in the diversification of ruminants in general,

346   and in the differences between bovids and cervids in particular.

347   The role of intrinsic constraints was assessed here by comparing various properties of the

348   within-population covariation ($\mathbf{P}$ and $\mathbf{P}_{AV}$; see table 1) with those of the among-population

349   divergence ($\mathbf{D}_{IC}$), where $\mathbf{P}$ is assumed to reflect the potential to evolve and diversify and $\mathbf{D}_{IC}$ reflects

350   the actual divergence that has occurred. Comparing $\mathbf{P}$ and $\mathbf{D}_{IC}$ in terms of their relative alignment

351   reveals that most species have their $\mathbf{P}$ matrices more closely aligned with the major axis of their

18

352   clade's D_{IC} than with any other direction (fig. 4). Cervids have lower evolvabilities along directions

353   in which they have diversified less than bovids, and higher evolvabilities in directions in which they

354   have diversified more than bovids (online fig. A12), again implying that intrinsic constraints have

355   influenced the directions in which bovids and cervids have diversified. In addition, species whose

356   divergence is more closely aligned with the direction of maximum evolvability have diverged

357   further away from their clade's ancestral state (fig. 5). At the same time, there is a great variation

358   in how well the **P** matrices of different species are aligned with divergence, implying also a great

359   variation among species in the orientation of their **P** matrices (fig. 4). This is in accord with a

360   previous analysis (Haber 2015), which found that closely-related taxa differ in the orientation of

361   their **P** matrices more than expected from their phylogenetic distance (assuming a single-rate

362   Brownian motion model) and that variation among bovid species in their matrix orientation is

363   similar to that among cervid species.

364   The positive signal in figures 4 and 5 is consistent with a role of intrinsic constraints in

365   ruminant diversification. However, without knowing the exact direction of selection throughout

366   the ruminant history, it is impossible to say whether the close alignment between **P** and D_{IC} is

367   because covariation has biased divergence or because selection has consistently pushed in the

368   direction of covariation. That said, in the time span included here – 25 My for bovids and 20 My for

369   cervids – it is not likely that selection would be pushing in the direction of **P** for that long unless **P**

370   itself has aligned with selection, and such alignment would likely be due to its constraining effect

371   (Jones et al. 2003; Revell 2007; Arnold et al. 2008). Therefore, although not conclusive, these

372   results suggest that the orientation and size of **P** have likely played a substantial role in

373   determining the direction and magnitude of ruminant divergence. Thus, this study joins others

374   (e.g., Hansen and Voje 2010) in demonstrating that even when covariance structure evolves

19

375   relatively rapidly, intrinsic constraints could still bias the evolution and divergence of populations.

376   At the same time, these analyses reveal little to no difference between bovids and cervids, and

377   therefore do not provide a good explanation for the finding that bovids' disparity is higher and

378   more evenly distributed than that of cervids.

379   The analyses presented in figures 4 and 5 focus on the relative alignment between

380   covariation and selection, accounting mostly for matrix orientation and size. As the time span and

381   phylogenetic scale of the study increase, it becomes more difficult to reconstruct this relative

382   alignment at any given time, and more likely that either or both have changed enough to obscure

383   their relative contribution. Moreover, from theoretical standpoint, additional considerations might

384   become more relevant on the macro scale, such as the heterogeneity of selection and the

385   probabilities of extinction and speciation (Vermeij 1973; Liem 1973; Jablonski 2007; Gomulkiewicz

386   and Houle 2009; Jones et al. 2012). Therefore, we might expect macroevolutionary patterns to be

387   predicted by properties that determine the potential of populations to respond effectively to a

388   wide range of challenges. Here, I considered four such measures: $\bar{e}, \bar{c}, \bar{f}$, and rSDE($\mathbf{P}$) (see table 1

389   for details). Each of these measures can be thought of as capturing – in its own way – the potential

390   of the population to respond relatively effectively to a wider range of selective pressures.

391   However, $\bar{c}$ has yielded different results depending on shrinking tolerance, method of matrix

392   inversion, and number of variables (online figure A3), due to its high sensitivity to sample size

393   (relative to number of variables) and strength of covariance. It is therefore considered less reliable

394   in this study, although this is not necessarily the case for conditional evolvabilities along specific

395   directions. $\bar{f}$ has a tight inverse correlation with rSDE($\mathbf{P}$) (fig. 1), in accord with expectations based

396   on the number of variables and heterogeneity of the matrices (see online Appendix B). Therefore,

20

397 in this study at least, these two metrics capture effectively the same information regarding the

398 potential to evolve into a wide range of directions. $\bar{e}$ is positively but loosely correlated with

399 rSDE(**P**) (fig. 1). Since rSDE(**P**) is scaled by matrix size, this result reflects more than just a scaling

400 association between the mean and variance of the eigenvalues. Instead, it suggests that as matrix

401 size increases, variance tends to be added more in directions with larger eigenvalues (thus

402 increasing the variance of the eigenvalues) rather than randomly or evenly.

403   The model-fitting results indicate that these properties have evolved within a relatively

404 limited range, which has shifted during the phylogenetic history of ruminants (fig. 2 and table 2).

405 The main shifts are found at the base of cervids and caprines for rSDE(**P**), and at the base of bovids

406 and caprines for $\bar{e}$ (online fig. A5). The high sigma-squared and alpha values (table 3) imply a great

407 lability and little phylogenetic signal among closely-related taxa. Yet, the fact that the observed

408 patterns are best explained by an Ornstein-Uhlenbeck model with multiple optima implies that

409 these properties have been relatively constrained at the family and subfamily scale in spite of a

410 great variation at the lower scales (Hansen 1997; Butler and King 2004). A good fit to the OU model

411 can also occur when a character evolves following Brownian motion with reflective barriers

412 (Harmon et al. 2010). rSDE(**P**) is indeed bound between 0 and 1, and $\bar{e}$ is bound by zero (even if log-

413 transformed for the model fitting), but there is no reason to expect them to be bound within a

414 different range for different subclades. Therefore, these findings suggest that rSDE(**P**) and $\bar{e}$ have

415 been under selection, either directly or indirectly, likely due to their association with morphological

416 diversification.

417   The maximum likelihood values inferred for rSDE(**P**) and $\bar{e}$ imply that bovids and cervids do

21

418   not share the same typical value for either of them. However, the value of $\bar{e}$ inferred for bovids is

419   very close to that of cervids, and even slightly lower. Based on the current theory, we would expect

420   the greater diversification of bovids to be associated with a higher average evolvability, rather than

421   a lower one, if constraints matter. Therefore, $\bar{e}$ cannot explain the greater diversificaton of bovids.

422   The values inferred for rSDE(**P**), on the other hand, are easier to interpret here, especially in

423   association with rSDE(**D**$_{IC}$). The value of rSDE(**P**) inferred for bovids – as well as the ruminant

424   ancestor – is lower than that of cervids (and independently, caprines; fig. 2 and table 3), suggesting

425   a greater potential to respond effectively to a wider range of selective pressures. Accordingly,

426   bovids have diversified into a wider range of directions in morphospace (a lower rSDE(**D**$_{IC}$)), in

427   addition to having a higher overall disparity (fig. 3). The finding that cervids have the same overall

428   rate of evolution as bovids even though their disparity is substantially lower (fig. 3) further

429   suggests that cervids' morphological evolution has been less diffusive than that of bovids, reverting

430   back to previously-explored areas more often. Therefore, these findings support a scenario in

431   which bovids have been able to take advantage of various ecological opportunities because they

432   have retained the low within-population eccentricity (and higher flexibility) that they had inherited

433   from their ancestor. Cervids, on the other hand, have taken the path of increasing eccentricity,

434   which has impeded their ability to take advantage of the same opportunities and channeled their

435   diversification.

436   Caprines dispersion is as spherical as that of other bovids (fig. 3) even though they have the

437   highest within-population eccentricity as a clade (fig. 2 and table 3). This implies that caprines'

438   evolutionary history does not follow the predicted association between rSDE(**P**) and rSDE(**D**$_{IC}$).

439   However, this apparent conflict may be explained by their early history. Caprines have been

22

440   identified as one of the most striking examples among ruminants of an explosive radiation

441   followed by high specialization (Geist 1985, 1987; Gentry 2000; Vrba and Schaller 2000; Ropiquet

442   and Hassanin 2005). Ropiquet and Hassanin (2005) point out that caprine diversification into tribes

443   concurs with the definition of adaptive radiation given by Schluter (2000): they have diversified

444   rapidly soon after the origination of their common ancestor in the late Miocene; they show great

445   morphological variation that follows a distinct environmental gradient; and their origination is

446   associated with a key innovation - short and stocky metacarpals - that has enabled them to invade

447   mountainous habitats not yet occupied by other herbivores. Thus, the exceptional diversification of

448   caprines is largely due to an early burst of rapid radiation. It is possible, therefore, that the lower

449   eccentricity – and higher flexibility – of their common ancestor had allowed it to take advantage of

450   the opening of a new kind of environment, diversify rapidly, and then specialize into a wide range

451   of climatic conditions. According to this scenario, the high eccentricity that characterizes some

452   caprines today has evolved only after their early burst of diversification, along with their

453   subsequent specialization.

454   The results presented here support the idea that the long-term evolutionary success of

455   lineages and clades is affected by their ability to respond effectively to a wide range of selective

456   pressures (Vermeij 1973; Liem 1973; Draghi and Wagner 2008). In addition, this study suggests that

457   the best predictor of that ability, at least in this case, is their within-population matrix shape,

458   measured as eccentricity (and/or average flexibility). However, the association found here

459   between rSDE(**P**) and macroevolutionary patterns, could also be a mere coincidence. More

460   empirical and theoretical work is required in order to establish the universality of these findings

461   and the validity of the additional assumptions underlying this association. Some empirical evidence

462   comes from research on morphological integration, to the extent that rSDE(**P**) reflects the

463   magnitude of integration. For example, Lower integration was found to be associated with greater

464   functional divergence in humans compared to apes (Rolian 2009; Rolian et al. 2010; Grabowski et

465   al. 2011) and higher module disparity in Carnivora (Goswami and Polly 2011). Some relevant

466   insights come from Draghi and Wagner (2008), who show that populations whose distribution of

467   mutational effects is less eccentric can adapt faster to a wider range of circumstances.

468   Several assumptions underlie the suggested association between matrix shape and

469   macroevolution. The main assumption is that selection changes frequently enough and in

470   directions different enough from the major axis of **P** (or **G**), thus providing the opportunities for

471   testing and realizing the potential reflected in matrix shape. This is ultimately an empirical

472   question. Recent metanalyses provide some evidence that evolutionary patterns across broad

473   taxonomic and time scales follow a model of erratic peak movements within fixed limits (Estes and

474   Arnold 2007; Uyeda et al. 2011). In addition, simulations could reveal how heterogeneous selection

475   needs to be in order for the potential to respond to a wide range of selective pressures to become

476   more relevant than the potential to respond faster in any particular direction. Another assumption

477   is that of a threshold that needs to be exceeded in order for the population to persist long enough

478   for an effective response. Gomulkiewicz and Houle (2009) developed formulae for calculating this

479   threshold, accounting for the structure of the fitness landscape and population dynamics. On the

480   macro scale, other factors probably contribute as well (Jablonski 2005, 2007, 2008). A yet another

481   assumption is that matrix shape (but not necessarily orientation or size) remains effectively stable

482   throughout the clade's history. This, again, is an empirical question for which there is currently too

483   little data. However, there is some evidence for it in the case of ruminants: pairwise comparisons

484   of matrix orientation have varied within 50% of their possible range (correlations of 0.4-0.9; Haber

485   2015), whereas eccentricity has varied within only 33% of its range (figs. 1 and 2). Simulations also

24

486   indicate that eccentricity tends to vary less than orientation under most combinations of genetic

487   architecture and selection regimes (Jones et al. 2003, 2012).

488   The association found here between matrix shape and ruminants' macroevolutionary

489   patterns implies a trade-off between the ability to respond effectively in a wide range of directions

490   and the ability to respond faster along a specific direction. This, in turn, implies a possible

491   dissociation between macro- and microevolution, where matrix eccentricity is associated with the

492   range and amount of clade dispersion on the macro scale, influenced by the heterogeneity of

493   selection, while matrix orientation and size are associated with the direction and magnitude of

494   population divergence relative to the direction and strength of selection on the generational scale.

495   Again, comprehensive simulations could reveal the range of parameters and conditions necessary

496   for this trade-off to occur. In addition, matrix shape could be linked to macroevolution through

497   taxonomic richness, if the probability of reproductive isolation increases when the population

498   moves in directions further away from the main axis of covariation (regardless of magnitude of

499   change) as opposed to moving along a narrow range of directions. This would be in accord with

500   other studies that point to a decoupling between population-level processes and

501   macroevolutionary patterns (Jablonski 2007 and references therein; Rabosky and Matute 2013).

502   Although the focus here is on macroevolutionary patterns, the same rationale should hold for

503   short-term evolution in highly dynamic environments, an issue that has become increasingly

504   relevant with the advance of global climate change (Kopp and Matuszewski 2013). Therefore,

505   studying variational properties that reflect the potential to respond to a wide range of selective

506   pressures could be useful also for understanding short-term population response to environments

507   with low predictability, as well as macroevolutionary patterns.

25

Literature cited

Ackermann, R. R., and J. M. Cheverud. 2002. Discerning evolutionary processes in patterns of

tamarin (genus *Saguinus*) craniofacial variation. American Journal of Physical Anthropology

117:260-271.

Agnarsson, I., and L. J. May-Collado. 2008. The phylogeny of Cetartiodactyla: The importance of

dense taxon sampling, missing data, and the remarkable promise of cytochrome b to

provide reliable species-level phylogenies. Molecular Phylogenetics and Evolution 48:964 -

985.

Allard, M. W., M. M. Miyamoto, L. Jarecki, F. Kraus, and M. R. Tennant. 1992. DNA systematics

and evolution of the artiodactyl family Bovidae. Proceedings of the National Academy of

Sciences of the United States of America 89:3972-3976.

Anderson, D. R., K. P. Burnham, and W. L. Thompson. 2000. Null hypothesis testing: problems,

prevalence, and an alternative. The Journal of Wildlife Management 64:912-923.

Armbruster, W. S. 1996. Evolution of floral morphology and function: an integrative approach to

adaptation, constraint, and compromise in *Dalechampia* (Euphorbiaceae). Pp. 241–272 *in* D.

Lloyd and S. C. H. Barrett, eds. Floral Biology. Chapman & Hall, New York.

Armbruster, W. S., C. Pélabon, G. H. Bolstad, and T. F. Hansen. 2014. Integrated phenotypes:

understanding trait covariation in plants and animals. Philosophical Transactions of the

Royal Society B: Biological Sciences 369

Arnold, S. J., R. Bürger, P. A. Hohenlohe, B. C. Ajie, and A. G. Jones. 2008. Understanding the

evolution and stability of the G-matrix. Evolution 62:2451-2461.

Arnold, S. J., M. E. Pfrender, and A. G. Jones. 2001. The adaptive landscape as a conceptual bridge

between micro- and macroevolution. Genetica 112-113:9-32.

Barber, C. B., K. Habel, R. Grasman, R. B. Gramacy, A. Stahel, and D. C. Sterratt. 2014. geometry: Mesh generation and surface tesselation.

Bolstad, G. H., T. F. Hansen, C. Pélabon, M. Falahati-Anbaran, R. Pérez-Barrales, and W. S. Armbruster. 2014. Genetic constraints predict evolutionary divergence in Dalechampia blossoms. Philosophical Transactions of the Royal Society B: Biological Sciences 369

Butler, M. A., and A. A. King. 2004. Phylogenetic comparative analysis: A modeling approach for adaptive evolution. American Naturalist 164:683-695.

Carpenter, J., and J. Bithell. 2000. Bootstrap confidence intervals: when, which, what? A practical guide for medical statisticians. Statistics in Medicine 19:1141-1164.

Cheverud, J. M., G. P. Wagner, and M. M. Dow. 1989. Methods for the comparative analysis of variation patterns. Systematic Zoology 38:201-213.

Decker, J. E., J. C. Pires, G. C. Conant, S. D. McKay, M. P. Heaton, K. Chen, A. Cooper, J. Vilkki, C. M. Seabury, A. R. Caetano, G. S. Johnson, R. A. Brenneman, O. Hanotte, L. S. Eggert, P. Wiener, J.-J. Kim, K. S. Kim, T. S. Sonstegard, T. Van, Curt P., H. L. Neibergs, J. C. McEwan, R. Brauning, L. L. Coutinho, M. E. Babar, G. A. Wilson, M. C. McClure, M. M. Rolf, J. Kim, R. D. Schnabel, and J. F. Taylor. 2009. Resolving the evolution of extant and extinct ruminants with high-throughput phylogenomics. Proceedings of the National Academy of Sciences 106:18644-18649.

DiCiccio, T. J., and B. Efron. 1996. Bootstrap Confidence Intervals. Statistical Science 11:189-212.

Draghi, J., and G. P. Wagner. 2008. Evolution of evolvability in a developmental model. Evolution 62:301-315.

Estes, S., and S. Arnold. 2007. Resolving the Paradox of Stasis: Models with Stabilizing Selection

Explain Evolutionary Divergence on All Timescales. The American Naturalist 169:227-244.

Foote, M. 1993. Discordance and concordance between morphological and taxonomic diversity. Paleobiology 19:185-204.

Geist, V. 1985. On evolutionary patterns in the Caprinae with comments on the punctuated mode of evolution, gradualism and a general model of mammalian evolution. Pp. 15-30 *in* S. Lovari, ed. The Biology and Management of Mountain Ungulates. Croom Helm Ltd, London.

Geist, V. 1987. On speciation in Ice Age mammals, with special reference to cervids and caprids. Canadian Journal of Zoology 65:1067–1084.

Gentry, A. W. 2000. The ruminant radiation. Pp. 11-25 *in* E. S. Vrba and G. B. Schaller, eds. Antelopes, Deer, and Relatives: Fossil Record, Behavioral Ecology, Systematics and Conservation. Yale University Press, New Haven.

Gilbert, C., A. Ropiquet, and A. Hassanin. 2006. Mitochondrial and nuclear phylogenies of Cervidae (Mammalia, Ruminantia): Systematics, morphology, and biogeography. Molecular Phylogenetics and Evolution 40:101-117.

Gomulkiewicz, R., and D. Houle. 2009. Demographic and Genetic Constraints on Evolution. The American Naturalist 174:E218-E229.

Grubb, P. 2002. Order Artiodactyla. Pp. 637-722 *in* D. E. Wilson and D. M. Reeder, eds. Mammal Species of the World. John Hopkins University Press, Baltimore.

Haber, A. 2011. A Comparative Analysis of Integration Indices. Evolutionary Biology 38:476-488.

Hansen, T. F. 1997. Stabilizing Selection and the Comparative Analysis of Adaptation. Evolution 51:1341-1351.

Hansen, T. F. 2012. Adaptive landscapes and macroevolutionary dynamics. Pp. 205-226 *in* R. Calsbeek and S. E., eds. The adaptive Landscape in Evolutionary Biology. Oxford University

Press, Oxford.

Hansen, T. F., and D. Houle. 2008. Measuring and comparing evolvability and constraint in multivariate characters. Journal of Evolutionary Biology 21:1201-1219.

Hansen, T. F., C. Pélabon, and D. Houle. 2011. Heritability is not Evolvability. Evol Biol Evolutionary Biology 38:258-277.

Hansen, T. F., and K. L. Voje. 2011. Deviation from the line of least resistance does not exclude genetic constraints: a comment on Berner et al. (2010). Evolution 65:1821-1822.

Harmon, L. J., J. B. Losos, J. T. Davies, R. G. Gillespie, J. L. Gittleman, B. W. Jennings, K. H. Kozak, M. A. McPeek, F. Moreno-Roark, T. J. Near, A. Purvis, R. E. Ricklefs, D. Schluter, I. Schulte, J. A., O. Seehausen, B. L. Sidlauskas, O. Torres-Carvajal, J. T. Weir, and A. Ø. Mooers. 2010. Early bursts of body size and shape evolution are rare in comparative data. Evolution 64:2385-2396.

Harmon, L. J., J. T. Weir, C. D. Brock, R. E. Glor, and W. Challenger. 2008. GEIGER: investigating evolutionary radiations

. Bioinformatics 24:129-131.

Hernández Fernández, M., and E. S. Vrba. 2005. A complete estimate of the phylogenetic relationships in Ruminantia: a dated species-level supertree of the extant ruminants. Biological Review 80:269-302

Heywood, J. J. N. 2010. Explaining patterns in modern ruminant diversity: contingency or constraint? Biological Journal of the Linnean Society 99:657-672.

Hipp, A. L., and M. Escudero. 2010. MATICCE: mapping transitions in continuous character evolution. Bioinformatics 26:132-133.

Hohenlohe, P. A., and S. J. Arnold. 2008. MIPoD: A Hypothesis-Testing Framework for

Microevolutionary Inference from Patterns of Divergence. The American Naturalist 171:366-385.

Jablonski, D. 2005. Mass extinctions and macroevolution. Paleobiology 31:192-210.

Jablonski, D. 2007. Scale and hierarchy in macroevolution. Palaeontology 50:87-109.

Jablonski, D. 2008. Biotic interactions and macroevolution: extensions and mismatches across scales and levels. Evolution 62:715-739.

Janis, C. M. 1989. A climatic explanation for patterns of evolutionary diversity in ungulate mammals. Palaeontology 32:463-481.

Janis, C. M. 1990. Correlation of cranial and dental variables with dietary preferences in mammals: a comparison of macropodoids and ungulates. Memoirs of the Queensland Museum 28:349-366.

Janis, C. M. 2008. An evolutionary history of browsing and grazing ungulates. Pp. 21-45 *in* I. J. Gordon and H. H. T. Prins, eds. The Ecology of Browsing and Grazing. Springer-Verlag, Berlin, Germany.

Jones, A. G., S. J. Arnold, and R. Bürger. 2003. Stability of the G-Matrix in a Population Experiencing Pleiotropic Mutation, Stabilizing Selection, and Genetic Drift. Evolution 57:1747-1760.

Jones, A. G., R. Bürger, S. J. Arnold, P. A. Hohenlohe, and J. C. Uyeda. 2012. The effects of stochastic and episodic movement of the optimum on the evolution of the G-matrix and the response of the trait mean to selection. Journal of Evolutionary Biology 25:2210-2231.

Jorjani, H., L. Klei, and U. Emanuelson. 2003. A Simple Method for Weighted Bending of Genetic (Co)variance Matrices. Journal of Dairy Science 86:677-679.

Kopp, M., and S. Matuszewski. 2014. Rapid evolution of quantitative traits: theoretical

31

perspectives. Evolutionary Applications 7:169-191.

Lande, R. 1979. Quantitative Genetic Analysis of Multivariate Evolution, Applied to Brain: Body Size Allometry. Evolution 33:402-416.

Liem, K. F. 1973. Evolutionary Strategies and Morphological Innovations: Cichlid Pharyngeal Jaws. Systematic Zoology 22:425-441.

Marcot, J. D. 2004. Evolutionary Radiations of Ruminantia. Pp. 278. Committee on Evolutionary Biology. University of Chicago, Chicago, Illinois.

Marcot, J. D. 2007. Molecular Phylogeny of Terrestrial Artiodactyls: Conflicts and Resolution. Pp. 4-18 *in* D. R. Prothero and S. E. Foss, eds. The Evolution of Artiodactyla. The Johns Hopkins University Press, Baltimore.

Marroig, G., and J. M. Cheverud. 2004. Cranial evolution in sakis (*Pithecia*, Platyrrhini) I: Interspecific differentiation and allometric patterns. American Journal of Physical Anthropology 125:266-278.

Marroig, G., L. Shirai, A. Porto, F. de Oliveira, and V. De Conto. 2009. The Evolution of Modularity in the Mammalian Skull II: Evolutionary Consequences. Evolutionary Biology 36:136-148.

Mendoza, M., C. M. Janis, and P. Palmqvist. 2002. Characterizing complex craniodental patterns related to feeding behaviour in ungulates: a multivariate approach. Journal of Zoology 258:223-246.

Paradis, E., J. Claude, and K. Strimmer. 2004. APE: Analyses of Phylogenetics and Evolution in R language. Bioinformatics 20:289-290.

Pavlicev, M., J. Cheverud, and G. Wagner. 2009. Measuring Morphological Integration Using Eigenvalue Variance. Evolutionary Biology 36:157-170.

Pitra, C., J. Fickela, E. Meijaard, and P. C. Groves. 2004. Evolution and phylogeny of old world deer.

32

Molecular Phylogenetics and Evolution 33:880–895.

Price, S. A., O. R. P. Bininda-Emonds, and J. L. Gittleman. 2005. A complete phylogeny of the whales, dolphins and even-toed hoofed mammals (Cetartiodactyla). Biological Reviews 80:445–473.

Rabosky, D. L., and D. R. Matute. 2013. Macroevolutionary speciation rates are decoupled from the evolution of intrinsic reproductive isolation in Drosophila and birds. Proceedings of the National Academy of Sciences 110:15354-15359.

Revell, L. J. 2007. Testing the genetic constraint hypothesis in a phylogenetic context: a simulation study. Evolution 61:2720-2727.

Revell, L. J. 2012. phytools: an R package for phylogenetic comparative biology (and other things). Methods in Ecology and Evolution 3:217-223.

Revell, L. J., and L. J. Harmon. 2008. Testing quantitative genetic hypotheses about the evolutionary rate matrix for continuous characters. Evolutionary Ecology Research 10:311-331.

Rolian, C. 2009. Integration and Evolvability in Primate Hands and Feet. Evolutionary Biology 36:100-117.

Ropiquet, A., and A. Hassanin. 2005. Molecular phylogeny of caprines (Bovidae, Antilopinae): the question of their origin and diversification during the Miocene. Journal of Zoological Systematics & Evolutionary Research 43:49-60.

Schluter, D. 1996. Adaptive Radiation Along Genetic Lines of Least Resistance. Evolution 50:1766-1774.

Schluter, D. 2000. The Ecology of Adaptive Radiation. Oxford University Press, New York, USA.

Semprebon, G., C. M. Janis, and N. Solounias. 2004. The diets of the Dromomerycidae (Mammalia:

Artiodactyla) and their response to Miocene vegetational change. Journal Of Vertebrate Paleontology 24:427-444.

Sinclair, A. R. E. 2000. Adaptation, niche partitioning, and coexistance of African Bovidae: clues to the past *in* E. S. Vrba and G. B. Schaller, eds. Antelopes, Deer, and Relatives: Fossil Record, Behavioral Ecology, Systematics, and Conservation. Yale University Press.

Sokal, R. R., and F. J. Rohlf. 1995. Biometry. W. H. Freeman and company, New York.

Spencer, L. M. 1997. Dietary adaptations of Plio-Pleistocene Bovidae: implications for hominid habitat use. Journal of Human Evolution 32:201-228.

Theodor, J. M., K. D. Rose, and J. Erfurt. 2005. Artiodactyla *in* K. D. Rose and D. J. Archibald, eds. The Rise of Placental Mammals. John Hopkins University Press, Baltimore.

Uyeda, J. C., T. F. Hansen, A. J. Arnold, and J. Pienaar. 2011. The million-year wait for macroevolutionary bursts. Proceedings of the National Academy of Sciences Proceedings of the National Academy of Sciences 108:15908-15913.

Van Valen, L. M. 1974. Multivariate structural statistics in natural history. Journal of Theoretical Biology 45:235-247.

Von den Driesch, A. 1976. A guide to the measurement of animal bones from archaeological sites. Peabody Museum Bulletin 1:1-136.

Vrba, E. S., and G. B. Schaller. 2000. Antelopes, Deer, and Relatives: Fossil Record, Behavioral Ecology, Systematics, and Conservation. Yale University Press

Wagner, G. P. 1984. On the eigenvalue distribution of genetic and phenotypic dispersion matrices: Evidence for a nonrandom organization of quantitative character variation. Journal of Mathematical Biology 21:77-95.

Zeng, Z.-B. 1988. Long-Term Correlated Response, Interpopulation Covariation, and Interspecific

Allometry. Evolution 42:363-374.

Table 1. Parameters and metrics included in this study, their symbols, and their interpretations

Symbol	Measure		Meaning
P	Pooled within-population phenotypic V/CV matrix; based on individuals and corrected for sex and subspecies mean		Variation and covariation of traits among individuals within a species
$\mathbf{P}_{AV}$	Average pooled within-population phenotypic V/CV matrix; based on individuals and corrected for species mean, as well as sex and subspecies		Variation and covariation of traits among individuals within a species, averaged across species within a clade.
$\mathbf{D}_{IC}$	Among-population phenotypic V/CV matrix; based on species means and corrected for phylogenetic correlation assuming Brownian-motion model (i.e., V/CV of independent contrasts; Revell et al. 2007)		Evolutionary rate matrix; rate of evolution and coevolution of traits among species within a clade
λ	An eigenvalue of **P** or $\mathbf{D}_{IC}$		
β	A vector of p elements, drawn randomly from a normal distribution with mean of zero and SD of one, normed to a unit length		Selection gradient; direction of selection operating on each trait independently of other traits
Average evolvability $\bar{e}$	The average mean-scaled phenotypic variance in **P**; Proportional to matrix size	$E\left[\beta^t \mathbf{P}\beta\right]$ or $E\left[\lambda(\mathbf{P})\right]$	The expected ability of the population to respond to selection in a random direction independently of other directions
Average conditional evolvability $\bar{c}$	The average mean-scaled phenotypic variance in **P**, accounting for trait covariances; Includes both matrix size and matrix shape	$E\left[\left(\beta^t \mathbf{P}^{-1}\beta\right)^{-1}\right]$	The expected ability of the population to respond to selection in a random direction, assuming stabilizing selection in other directions
Average flexibility $\bar{f}$	Cosine of the angle between β and the response vector, averaged over random vectors; Matrix shape only	$E\left[\dfrac{\beta^t \mathbf{P}\beta}{\sqrt{\Sigma(\mathbf{P}\beta)^2}}\right]$	The expected ability of the population to track in the direction of selection; reflecting the range of random directions into which the population can potentially evolve with relative precision
Within-pop. Eccentricity rSDE(**P**)	Relative standard deviation of the eigenvalues of **P***; Matrix shape only	$\sqrt{\dfrac{p\sum(\lambda_i - \bar{\lambda})^2}{(p-1)\sum\lambda\sum\lambda}}$	The relative ability to track in different directions; reflecting the range of orthogonal directions into which the population can potentially evolve with relative precision
Among-pop. eccentricity rSDE($\mathbf{D}_{IC}$)	Relative standard deviation of the eigenvalues of $\mathbf{D}_{IC}$		Eccentricity of dispersion; the range of directions in space into which the species have diverged
$\mathbf{d}_{CL}$	An eigenvector of $\mathbf{D}_{IC}$		Direction of clade's dispersion
$\mathbf{d}_{SP}$	Difference vector between a species mean and its clade's phylogenetically-weighted mean (inferred root state) assuming Brownian motion, standardized by that mean and normed to a unit length.		Direction of morphological divergence between a species and its clade's ancestral state
d^2	Squared distance between a species mean and its clade's inferred root	$\mathbf{d}_{sp}{}^t\,\mathbf{d}_{sp}$	Amount of morphological divergence between a species and its clade's ancestral state
Disparity	Average distance between species means and the clade's inferred root	$\dfrac{\sum d^2}{(N_{sp}-1)}$	Total amount of clade's dispersion
	Trace of $\mathbf{D}_{IC}$		Rate of dispersion
$e(\mathbf{d}_{SP})$	Mean-scaled phenotypic variance in the direction of species divergence	$\mathbf{d}_{sp}{}^t\,\mathbf{P}_{av}\,\mathbf{d}_{sp}$	The variation available for species, on average, in the direction of their divergence
$c(\mathbf{d}_{SP})$	Mean-scaled phenotypic variance in the direction of species divergence, accounting for trait covariances	$E\left[\dfrac{1}{\mathbf{d}_{sp}{}^t\,\mathbf{P}_{av}{}^{-1}\,\mathbf{d}_{sp}}\right]$	The variation available for species, on average, in the direction of their divergence assuming stabilizing selection in other directions
$e(\mathbf{d}_{CL})$	Mean-scaled phenotypic variance available along the eigenvectors of $\mathbf{D}_{IC}$	$\mathbf{d}_{CL}{}^t\mathbf{P}\mathbf{d}_{CL}$	The variation available for each species in the direction of their clade's diversification

* p is number of traits
** N_{SP} is number of species

Table 2. The different models describing the evolution of of rSDE(**P**), and $\bar{e}$. Based on the IL32 dataset. The best-supported models are in bold. K is the number of parameters in the model.

Model No.	K	Nodes included in the model (1)					rSDE(**P**)		$\bar{e}$	
		8FV*	Cervidae	Cervinae	Bovidae	Caprinae	AICc scores	AICc weights	AICc scores	AICc weights
1	8	1	1	1	1	1	93.24	0.0096	11.11	0.0045
2	7	0	1	1	1	1	90.42	0.0392	8.28	0.0186
3	7	1	0	1	1	1	90.42	0.0392	8.28	0.0186
4	6	0	0	1	1	1	90.07	0.0466	6.08	0.0561
5	7	1	1	0	1	1	91.79	0.0197	8.31	0.0184
6	6	0	1	0	1	1	89.10	0.0759	5.62	0.0707
7	6	1	0	0	1	1	89.10	0.0759	5.62	0.0707
8	5	0	0	0	1	1	89.87	0.0517	**3.50**	**0.2032**
9	7	1	1	1	0	1	90.42	0.0392	8.28	0.0186
10	6	0	1	1	0	1	**87.74**	**0.1497**	8.51	0.0166
11	6	1	0	1	0	1	94.17	0.0060	10.12	0.0074
12	5	0	0	1	0	1	91.65	0.0212	9.35	0.0110
13	6	1	1	0	0	1	89.10	0.0759	5.62	0.0707
14	5	0	1	0	0	1	**86.54**	**0.2728**	5.96	0.0594
15	5	1	0	0	0	1	96.02	0.0024	8.69	0.0152
16	4	0	0	0	0	1	93.73	0.0075	7.81	0.0236
17	7	1	1	1	1	0	98.92	0.0006	12.79	0.0020
18	6	0	1	1	1	0	96.22	0.0022	10.09	0.0075
19	6	1	0	1	1	0	96.22	0.0022	10.09	0.0075
20	5	0	0	1	1	0	95.01	0.0039	7.97	0.0218
21	6	1	1	0	1	0	97.43	0.0012	10.12	0.0074
22	5	0	1	0	1	0	94.85	0.0043	7.54	0.0270
23	5	1	0	0	1	0	94.85	0.0043	7.54	0.0270
24	4	0	0	0	1	0	94.65	0.0047	5.51	0.0747
25	6	1	1	1	0	0	96.22	0.0022	10.09	0.0075
26	5	0	1	1	0	0	93.69	0.0076	9.58	0.0097
27	5	1	0	1	0	0	96.03	0.0024	10.18	0.0072
28	4	0	0	1	0	0	93.73	0.0075	9.15	0.0121
29	5	1	1	0	0	0	94.85	0.0043	7.54	0.0270
30	4	0	1	0	0	0	92.43	0.0144	7.14	0.0330
31	4	1	0	0	0	0	96.83	0.0016	8.50	0.0167
32	3	0	0	0	0	0	94.76	0.0045	7.43	0.0285
BM	2	0	0	0	0	0	102.01	0.0001	36.35	0.0000

*8FV – Node No. 8 in Hernández Fernández and Vrba (2005), including Bovidae plus Cervidae without Tragulidae

36

Table 3. Maximum likelihood estimates for the best-supported models for the evolution of rSDE(**P**), and $\bar{e}$ (see table 2 and online table A3). Nodes for which a transition was inferred are in bold. Estimates for Brownian motion (BM) model are also given. Average values are weighted by AIC weights. All data are mean-scaled. Branch length is scaled by tree height. Theta values of rSDE(**P**) are adjusted for sample size as in fig. 1.

	Dataset	Model No.	Theta 8FV	Cervidae	Cervinae	Bovidae	Caprinae	Alpha	Sigma-squared
Within-pop. Eccentricity rSDE(**P**)	IL32 *	14	0.07	**0.15**	0.15	0.07	**0.16**	9.67	5.23
		10	0.07	**0.13**	**0.20**	0.07	**0.16**	9.61	5.06
		Average	0.09	**0.14**	0.16	0.07	**0.15**	8.96	4.91
		BM			0.08			--	1.38
	ILtes †	14	0.15	**0.23**	0.23	0.15	**0.31**	9.48	2.48
		10	0.15	**0.21**	**0.28**	0.15	**0.31**	9.21	2.36
		Average	0.17	**0.21**	0.24	0.15	**0.31**	8.64	2.29
		BM			0.16			--	0.66
Average evolvability $\bar{e}$	IL32 *	8	0.0057	0.0057	0.0057	**0.0048**	**0.0061**	70.45	7.13
		Average	0.0065	0.0056	0.0057	**0.0049**	**0.0057**	113.62	12.17
		BM			0.0055			--	0.38
	ILtes †	8	0.0050	0.0050	0.0050	**0.0040**	**0.0060**	34.28	3.69
		14	0.0040	**0.0050**	0.0050	0.0040	**0.0060**	33.59	3.75
		Average	0.0054	0.0049	0.0050	**0.0040**	**0.0059**	32.88	3.57
		BM			0.0046			--	0.37

* Reduced dataset of 32 interlandmark distances

† Tessellation-based dataset of 107 interlandmark distances

37

Figure legends

Figure 1: Comparison of **P**-matrix properties based on the IL32 dataset, mean-scaled. See table 1 for details on how these properties are measured and interpreted. Solid line indicates regression line. Grey bars indicate 95% confidence intervals based on non-parametric bootstrap with BCa correction.

Figure 2. The relative standard deviation of eigenvalues (rSDE(**P**)) calculated for the IL32 dataset, mean-scaled. Values were adjusted for sample size by subtracting the mean permutation value from the observed value. Therefore, zero represents the expected value for a random matrix. Sample sizes are given in parentheses. Phylogenetic relationships follow Hernandez-Fernandez and Vrba (2005). Vertical dashed lines represent the maximum likelihood estimates (see table 3).

Figure 3. Measures of diversification for the four clades that involve a shift in their typical within-population eccentricity (see figure 1 and table 2), based on the IL32 dataset. Their inferred rSED(**P**) and $\bar{e}$ values are also shown (see table 3). All metrics are proportional to the clade's phylogenetically-weighted mean. Bars in the top panel (disparity) represent the expected distribution under Brownian motion model (95% interval). Bars in the lower two panels (rates and eccentricity) represent 95% confidence interval. Analyses involving Cervidae were repeated with (cross) and without (circle) *Alces*. Analyses involving Bovidae were repeated with (cross) and without (circle) Caprinae.

Figure 4: Evolvabilities in directions of clade's diversification ($e(\mathbf{d}_{CL})$), measured as the amount of variation that each species has in its **P**-matrix in the direction of its clade's eigenvectors. Eigenvectors are ordered by the relative size of their eigenvalues, indicated along the x-axis.

Figure 5: Evolvabilities ($e(\mathbf{d}_{sp})$) and conditional evolvabilities ($c(\mathbf{d}_{sp})$) in the direction of species divergence, calculated based on the average within-species covariance matrix ($\mathbf{P}_{AV}$), plotted against the amount of divergence between each species and its clade's ancestral state (d^2). Everything is proportional to trait mean. d^2 is ln-transformed for clarity. Horizontal bars mark the minimum and maximum evolvabilities (solid), the expected evolvability ($\bar{e}$, dashed) and conditional evolvability ($\bar{c}$, dotted). Caprines are highlighted in black in the top graph. Based on IL32
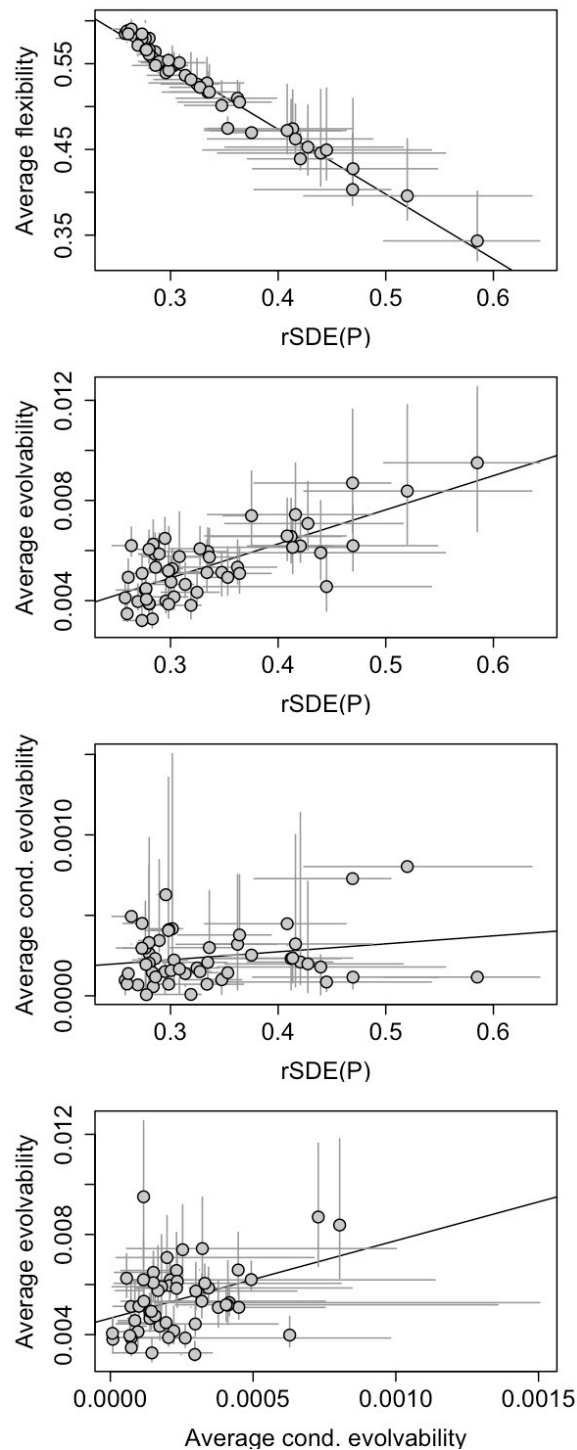
Figure 1: Comparison of **P**-matrix properties based on the IL32 dataset, mean-scaled. See table 1 for details on how these properties are measured and interpreted. Solid line indicates regression line. Grey bars indicate 95% confidence intervals based on non-parametric bootstrap with BCa correction.
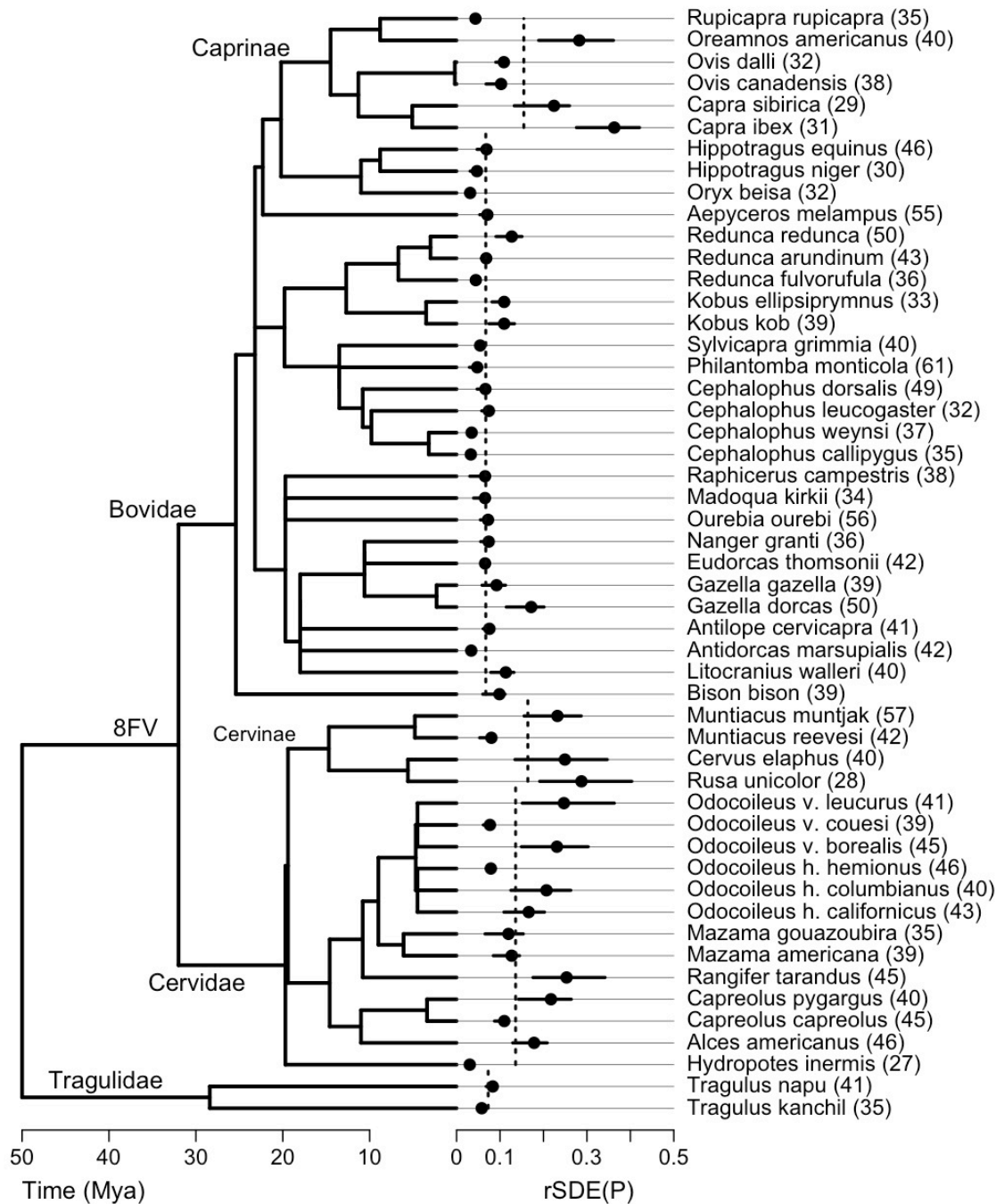
Figure 2. The relative standard deviation of eigenvalues (rSDE(**P**)) calculated for the IL32 dataset, mean-scaled. Values were adjusted for sample size by subtracting the mean permutation value from the observed value. Therefore, zero represents the expected value for a random matrix. Sample sizes are given in parentheses. Phylogenetic relationships follow Hernandez-Fernandez and Vrba (2005). Vertical dashed lines represent the maximum likelihood estimates (see tables 2 and 3).
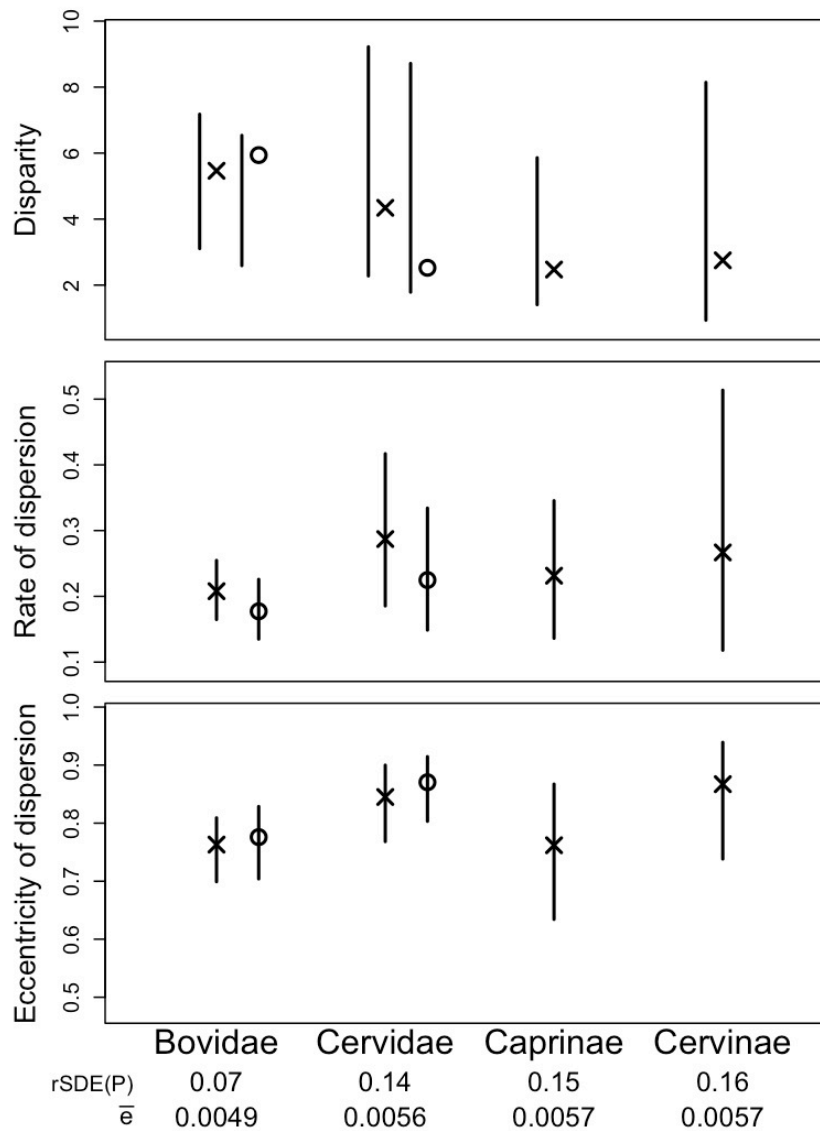
40

	Bovidae	Cervidae	Caprinae	Cervinae
rSDE(P)	0.07	0.14	0.15	0.16
$\bar{e}$	0.0049	0.0056	0.0057	0.0057

Figure 3. Measures of diversification for the four clades that involve a shift in their typical within-population eccentricity (see figure 1 and table 2), based on the IL32 dataset. Their inferred rSED(**P**) and $\bar{e}$ values are also shown (see table 3). All metrics are proportional to the clade's phylogenetically-weighted mean. Bars in the top panel (disparity) represent the expected distribution under Brownian motion model (95% interval). Bars in the lower two panels (rates and eccentricity) represent 95% confidence interval. Analyses involving Cervidae were repeated with (cross) and without (circle) *Alces*. Analyses involving Bovidae were repeated with (cross) and without (circle) Caprinae.
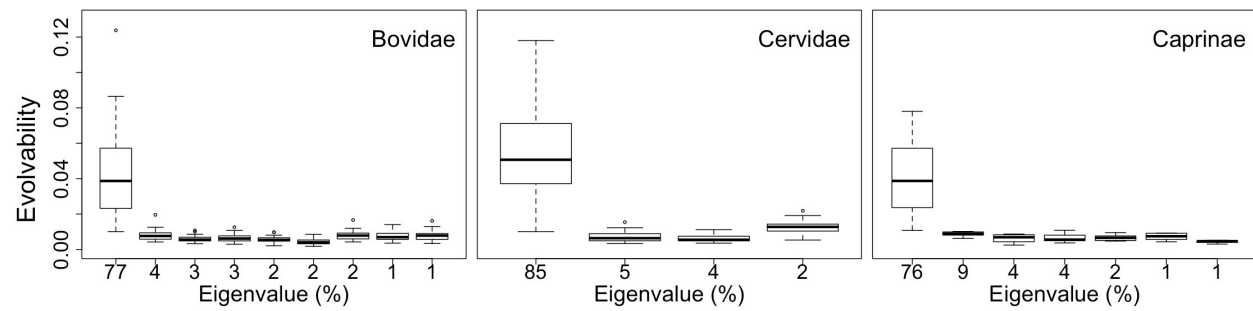
41

Figure 4: Evolvabilities in directions of clade's diversification ($e(\mathbf{d}_{CL})$), measured as the amount of variation that each species has in its **P**-matrix in the direction of its clade's eigenvectors. Eigenvectors are ordered by the relative size of their eigenvalues, indicated along the x-axis.
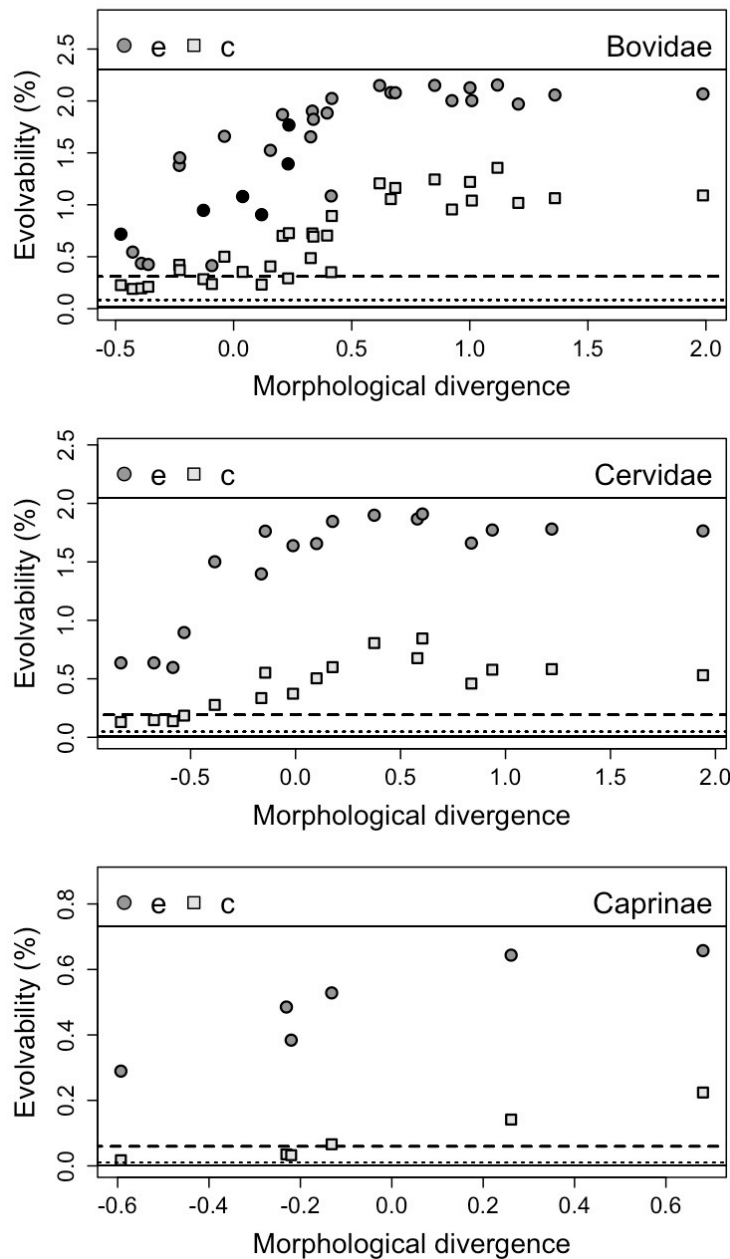
Figure 5: Evolvabilities ($e(\mathbf{d}_{sp})$) and conditional evolvabilities ($c(\mathbf{d}_{sp})$) in the direction of species divergence, calculated based on the average within-species covariance matrix ($\mathbf{P}_{AV}$), plotted against the amount of divergence between each species and its clade's ancestral state (d^2). Everything is proportional to trait mean. d^2 is ln-transformed for clarity. Horizontal bars mark the minimum and maximum evolvabilities (solid), the expected evolvability ($\bar{e}$, dashed) and conditional evolvability ($\bar{c}$, dotted). Caprines are highlighted in black in the top graph. Based on IL32